Journal of Materials Chemistry C

Diversifying Peripheral Aromatic Units of Pyrrolo[3,2-b]pyrrole-Containing Conjugated Polymers and the Resulting Optoelectronic Properties

Journal:	*Journal of Materials Chemistry C*
Manuscript ID	TC-ART-01-2025-000292.R2
Article Type:	Paper
Date Submitted by the Author:	13-Mar-2025

Complete List of Authors:	Collier, Graham; University of Southern Mississippi, School of Polymer Science and Engineering; Kennesaw State University, Department of Chemistry and Biochemistry Layton, Julien T.; Kennesaw State University, Department of Chemistry and Biochemistry Skiouris, Perry; University of Southern Mississippi, School of Polymer Science and Engineering Wagner, Ethan W.; Kennesaw State University, Department of Chemistry and Biochemistry Phan, Vanessa; University of Southern Mississippi, School of Polymer Science and Engineering Fraser, Sarah ; University of North Georgia, Department of Chemistry and Biochemistry Bell, Kenneth-John; Kennesaw State University, Deparment of Chemistry and Biochemistry Tomlinson, Aimée; University of North Georgia, Department of Chemistry and Biochemistry

Diversifying Peripheral Aromatic Units of Pyrrolo[3,2-*b*]pyrrole-Containing Conjugated Polymers and the Resulting Optoelectronic Properties

Graham S. Collier[a,b]*, Julien T. Layton,[b] Perry Skiouris,[a] Kenneth-John J. Bell,[b] Ethan W. Wagner,[b] Vanessa Phan,[a] Sarah G. Fraser[c], and Aimée L. Tomlinson[c]

[a]Center for Optoelectronic Materials and Devices, School of Polymer Science and Engineering, University of Southern Mississippi, Hattiesburg, MS, 39406, USA

[b]Department of Chemistry and Biochemistry, Kennesaw State University, Kennesaw GA, 30144, USA

[c]Department of Chemistry and Biochemistry, University of North Georgia, Dahlonega, GA, 30597, USA

Abstract

Utilizing synthetically-simple monomers to create conjugated polymers with tailorable properties is important for continued development of materials suited for organic electronics. Pyrrolo[3,2-*b*]pyrrole (DHPP) has been shown to reduce the synthetic complexity commonly associated with conjugated polymers but tailoring properties was limited to choice of comonomer that is coupled with phenyl-containing DHPPs. Here, the DHPP monomer toolbox is diversified to include thienyl and benzothiadiazole aromatic units directly attached to the periphery of DHPP monomers. Dibrominated monomers are polymerized via Suzuki cross-coupling polymerizations to generate a series of DHPP "homopolymers" with tailorable optoelectronic properties. While phenyl- and thienyl-containing polymers demonstrate localized excitation properties, the benzothiadiazole-containing DHPP polymer exhibits charge-transfer character associated with donor-acceptor materials. These differences in the aromatic unit enables optical absorbances to be tuned across the visible spectrum and provides design guidelines for attaining electrochemically stable DHPP polymers. In addition to fundamental insights into structure-property relationships of DHPP-based polymers, the synthetic simplicity and tailorability of DHPPs continues to motivate using these building blocks in conjugated materials for optical and electronic devices.

Introduction

The ability to systematically manipulate properties through structural alterations continues to inspire researchers to study conjugated polymers for a variety of applications including, but not limited to, organic photovoltaics (OPVs),[1] organic light-emitting diodes (OLEDs),[2] electrochromics,[3] and bioelectronics.[4] While the structural design motifs that may be useful for accessing conjugated materials deemed "high-performing" seem to only be limited by one's imagination, the synthetic approaches used to access such materials is often quite complex, requires numerous steps, and generates large amounts of chemical waste.[5–7] As such, there is a growing desire for the field to pursue conjugated polymers with simple structures and synthetic pathways, tunable optoelectronic properties, and high-performance metrics in device-inspired measurements such as conductivity or power conversion efficiency (PCE).[8]

As the field of conjugated polymers evolved, poly(3-hexylthiophene) (P3HT) has served as a benchmark material arguably due to availability from a reproducible, scalable, and rather simple synthesis.[9,10] Despite the popularity of P3HT, and the impact it has had on understanding phenomenon governing polymer performance, the modest device[11,12] performance metrics with fullerene or non-fullerene acceptors dampens enthusiasm for this polymer to realize commercial success. This dwindling enthusiasm has led to the development of donor-acceptor (D-A) type copolymers that push the limits of device performance but has simultaneously increased the synthetic complexity of the polymers.[6] For example, a donor polymer notated as D18 achieved a PCE over 18% when blended with the non-fullerene acceptor Y6[13] but suffers low overall yields from 10 synthetic steps for *one* monomer.[14] This challenging synthesis motivated the You group to explore new synthetic protocols that ultimately led to improved overall yields but still required 12 synthetic steps to prepare a necessary monomer.[15] There are examples of D-A copolymers that

have rather simple synthetic protocols without sacrificing performance metrics. For example, the polymer PTQ-10 can be synthesized in 3 synthetic steps and achieves PCEs of 19% when blended with a non-fullerene acceptor.[16–18] These attributes have motivated researchers to pursue more cost-effective synthesis[19] and expand side chain functionality that enables green solvent processing[20] but synthesis still requires using Stille cross-coupling polymerizations that produce stoichiometric amounts of potentially toxic waste. Other recent efforts by the Heeney group have involved utilizing scalable nucleophilic aromatic substitution (SN_{Ar}) protocols to attain simple D-A polymers with tunable structures and solubility in conjunction with respectable PCEs.[21] As it relates to redox-active polymers, propylenedioxythiophene (ProDOT)-based polymers are the benchmark for the field due to their outstanding optical contrast,[22,23] electrochemical stability,[24] and diverse applicability. The utility of ProDOT polymers is supported by diverse, simple, and scalable syntheses[25,26] and monomers have even been shown to be amenable to continuous flow chemistry.[27] Each of these systems represent respectable advancements in the synthesis science of conjugated polymers and provide inspiration to find new structures that further simplify the preparation of these materials.

When envisioning other building blocks that may be useful for attaining structurally-diverse conjugated materials via simple syntheses, 1,4-dihydropyrrolo[3,2-*b*]pyrroles (DHPPs) garner attention due to their ease of synthesis and expansive design space facilitated by the variety of readily available aromatic aldehydes and anilines.[28] The synthesis involves an Fe-catalyzed multicomponent reaction (MCR) that is performed in a single aerobic step and purification is typically achieved via vacuum filtration.[29,30] Ultimately, these chromophores have been used as the active layer material in OPVs or dye-sensitized solar cells (DSSCs),[31,32] emissive material in OLEDs,[33] as organic linkers in responsive metal-organic-frameworks (MOFs),[34] and more recently

as color-controlled high-contrast electrochromes.[35] Their ease of synthesis and structural tailorability ultimately motivated our group to begin incorporating DHPPs into the main chain repeat unit of conjugated polymers via Pd-catalyzed cross-coupling[36,37] or acid-catalyzed condensation polymerizations.[38] Overall, our efforts led to a quantitative reduction in the synthetic complexity commonly associated with conjugated polymers while demonstrating high-contrast or multi-colored electrochromism,[39] PCEs ~2.5% with hole mobilities similar to high-performing copolymers, or on-demand acid-catalyzed degradation. While our polymer systems demonstrate the ability to enchain DHPP monomers into a polymer repeat unit, the aromatic units directly adjacent to the DHPP core were relegated to benzene rings. The increased aromaticity in the benzene ring inhibits efficient formation of the quinoidal structure of the conjugated polymer and introduces large dihedral angles, both of which are detrimental to properties such as mobility and optical contrast upon doping. Furthermore, benzene-based electrochromes are hypothesized the be susceptible to undesired side reactions when doped that lead to decreased stability with extended switching protocols.[40] As such, there is motivation to broaden the structural-diversity of the aromatic functionalities at the periphery of DHPPs monomers that will enable further tunability of polymer properties while also enhancing performance metrics.

Motivation for diversifying aromatic functionality at the DHPP periphery is gained from the molecular DHPP literature. First, in their seminal reports of the Fe-catalyzed MCR to synthetize DHPPs, the Gryko group reported being able to incorporate electron-rich aromatics to the DHPP scaffold resulting in large fluorescence quantum yields and red-shifted absorbance/emission spectra compared to tetraphenyl-DHPPs.[29] This same group also showed that aromatic functionality and positioning of a nitro group influence intersystem crossing of quadrapolar DHPPs.[41] Beyond fundamental studies into structure-property relationships,

heteroaromatic moieties offer useful attributes across many applications. For example, Ippolito and coworkers synthesized a thienyl-functionalized DHPP that was used in a single component, wide broadband photodetector.[42] Pyridyl-functionalized DHPPs have been used as probes for nuclei cell imaging[43,44] or as coordinating N→B bonds that locks DHPP chromophores in a planar conformation that ultimately yields deep red emission upon photoexcitation.[45] DHPPs functionalized with coumarins[46] or tetrazolo[1,5-*a*]quinolines[47] generate strongly polarized chromophores that display strong two photon absorbance. Finally, thiazole-functionalized DHPPs facilitate further modifications that enable eliminating the large dihedral angles associated with phenyl-functionalized DHPPs and leads to a new approach for manipulating optoelectronic properties of DHPP chromophores.[48]

Motivated by the successes of the reported molecular systems, and as alluded to in Figure 1, we were interested to explore how properties change when DHPP monomers, and subsequently polymers, are designed with differing peripheral aromatic units. Herein, we report the synthesis of phenyl-, thienyl-, and benzothiadiazole-functionalized DHPP monomers via an Fe-catalyzed multicomponent reaction that readily participate in Pd-catalyzed Suzuki cross-coupling polymerizations. The resulting polymers expand the structural diversity of a class of synthetically-simple conjugated polymers and leads to straightforward manipulation of optoelectronic properties. Specifically, the thienyl- and benzothiadiazole-containing polymers display distinct red shifts in their absorbance spectra compared to a phenyl-containing polymer in solution and as thin films that are attributed to increased planarization along the polymer backbone and enhanced intramolecular charge transfer processes, respectively. Thermal characterization via thermal gravimetric analysis reveals the polymers to have excellent thermal stability while differential scanning calorimetry results indicate the polymers are amorphous evident by the absence of

distinct thermal transitions. Electrochemical properties, measured via cyclic voltammetry (CV) and spectroelectrochemistry, reveal redox properties and stability to be strongly influenced by repeat unit composition. This study represents an expansion to monomer design considerations for the synthetically-simple DHPP system that enables systematic manipulation of polymer properties and offers enhanced performance metrics, such as improved redox stability. Overall, the results presented here represent a continued demonstration of DHPP being a useful building block for attaining conjugated systems with simplified synthesis while possessing properties that will be useful as next-generation organic electronic materials.

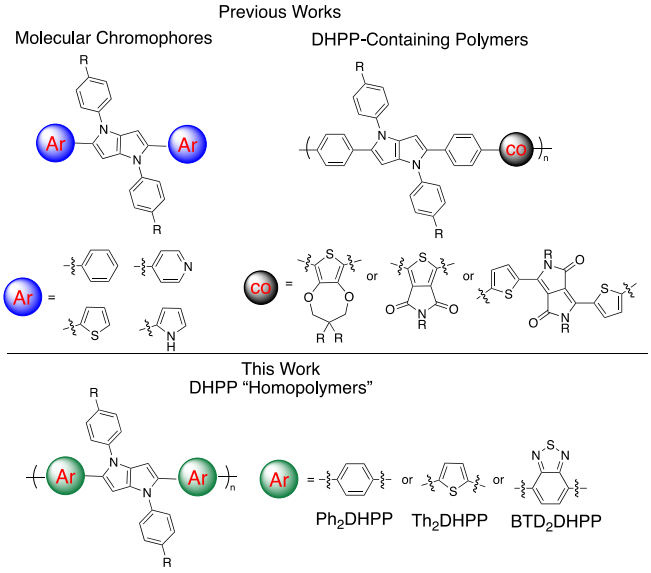

Figure 1. Representative evolution of DHPP-containing chromophores and polymers.

Results and Discussion

Monomer and Polymer Synthesis and Characterization

DHPP-containing polymers are known to have limited solubility in common organic solvents which has required synthesizing customized anilines with branched side chains. To ensure solubility of the resulting DHPP polymers, DHPP monomers were synthesized by reacting anilines functionalized with branched hexyldecyl side chains with 4-bromobenzaldehyde, 5-bromo-2-

thiophenecarbaldehyde, or 7-bromobenzo[*c*][1,2,5]thiadiazole-4-carbaldehyde followed by the addition of 2,3-butanedione and $Fe(ClO_4)_3$ to attain *m*-Ph_2DHPP, *m*-Th_2DHPP, and *m*-BTD_2DHPP, respectively (Scheme 1(A)). The monomer *m*-Ph_2DHPP readily precipitated from the crude reaction mixture which enabled collection via vacuum filtration and purification by washing with cold MeOH and acetone to attain the desired monomer in 47% yield. The monomers *m*-Th_2DHPP and *m*-BTD_2DHPP required modifications to the purification protocols. Purifying *m*-Th_2DHPP required precipitating the crude reaction mixture into cold MeOH to yield a brown sludge. The brown sludge was collected via vacuum filtration and subsequently washed with cold MeOH and acetone until a pale-yellow solid remained. The pale-yellow solid was collected in 15% yield and was confirmed to be the desired thienyl-functionalized monomer. The lower yield for *m*-Th_2DHPP compared to *m*-Ph_2DHPP is common for electron-rich DHPPs and likely stems from the stabilization of the imine that is formed during the beginning stages of the multicomponent reaction. The monomer *m*-BTD_2DHPP precipitated into cold MeOH as an amorphous solid that clogged the filter during attempts to isolate the product. The pure monomer could ultimately be obtained in 12% yield after recrystallizing the crude product from ethyl acetate.

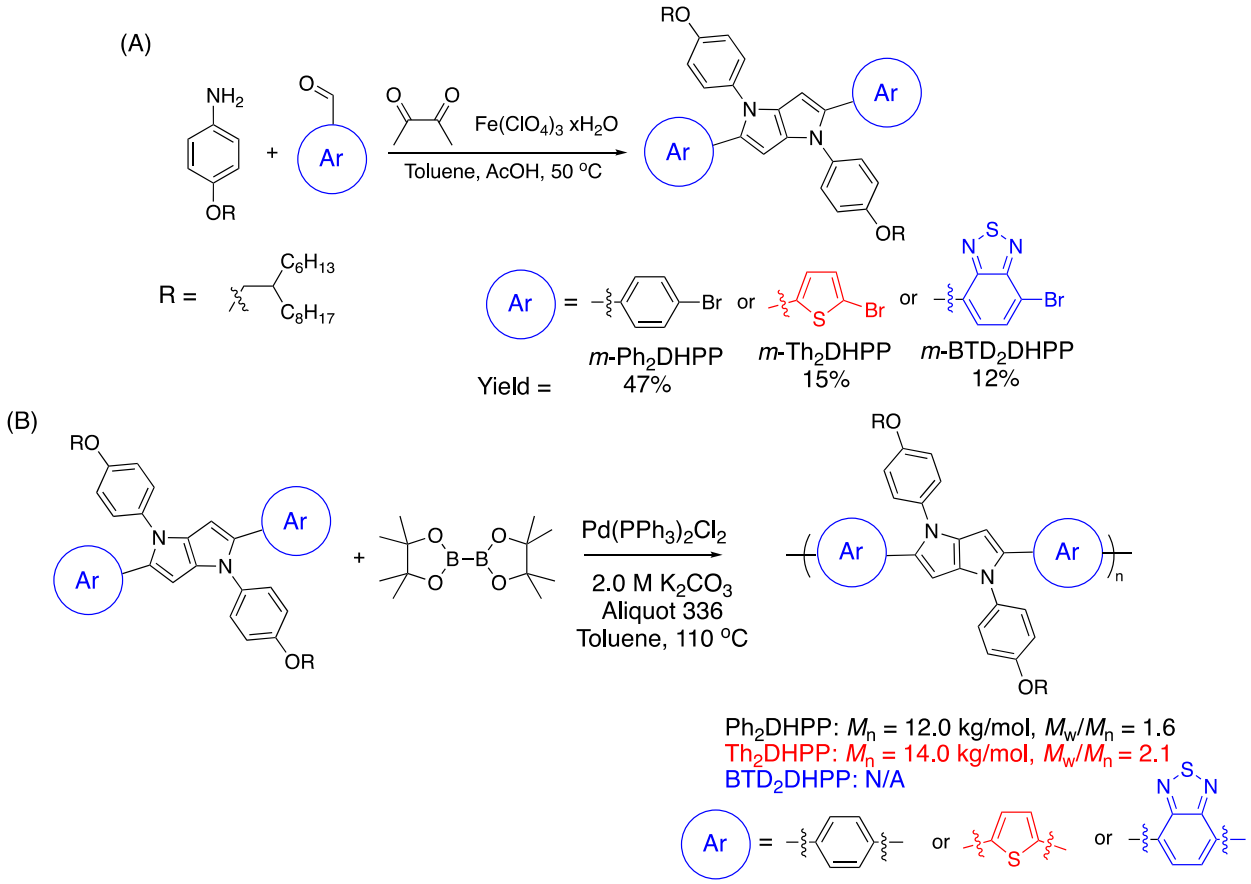

Scheme 1. (A) Synthesis of dihalogenated monomers via the Fe(III)-catalyzed multicomponent reaction. (B) Suzuki polymerizations of DHPP monomers with bis(pinacolato)boron for the synthesis of DHPP-containing polymers.

Characterization of the DHPP monomers via ^{1}H NMR revealed differences in the aromatic chemical shifts based on the choice of peripheral aromatic unit, as represented by the spectra presented in Figure 2. The chemical shift associated with the 3,6-protons of the DHPP core serves as the diagnostic peak for the DHPP molecules with *m*-Ph$_2$DHPP appears at 6.34 ppm while the same peak for *m*-Th$_2$DHPP appears at 6.23 ppm. The difference is attributed to the thiophene being more electron rich than the phenyl group that leads to increased proton shielding. Alternatively, the diagnostic peak for *m*-BTD$_2$DHPP shows a drastic downfield shift to 7.01 ppm due to the electron-deficient BTD leading to increased deshielding of the DHPP core protons. This same phenomenon has been observed for donor-acceptor purine-based chromophores[49] and supported

the intuition that electronic properties were susceptible changes based on the choice of aromatic linker. The different electron distributions in this study support the notion that optoelectronic properties of the resulting DHPP-containing polymers can be tuned based on the identity of the peripheral aromatic group similar to substituent effects previously reported by our group for molecular DHPPs.[35,39]

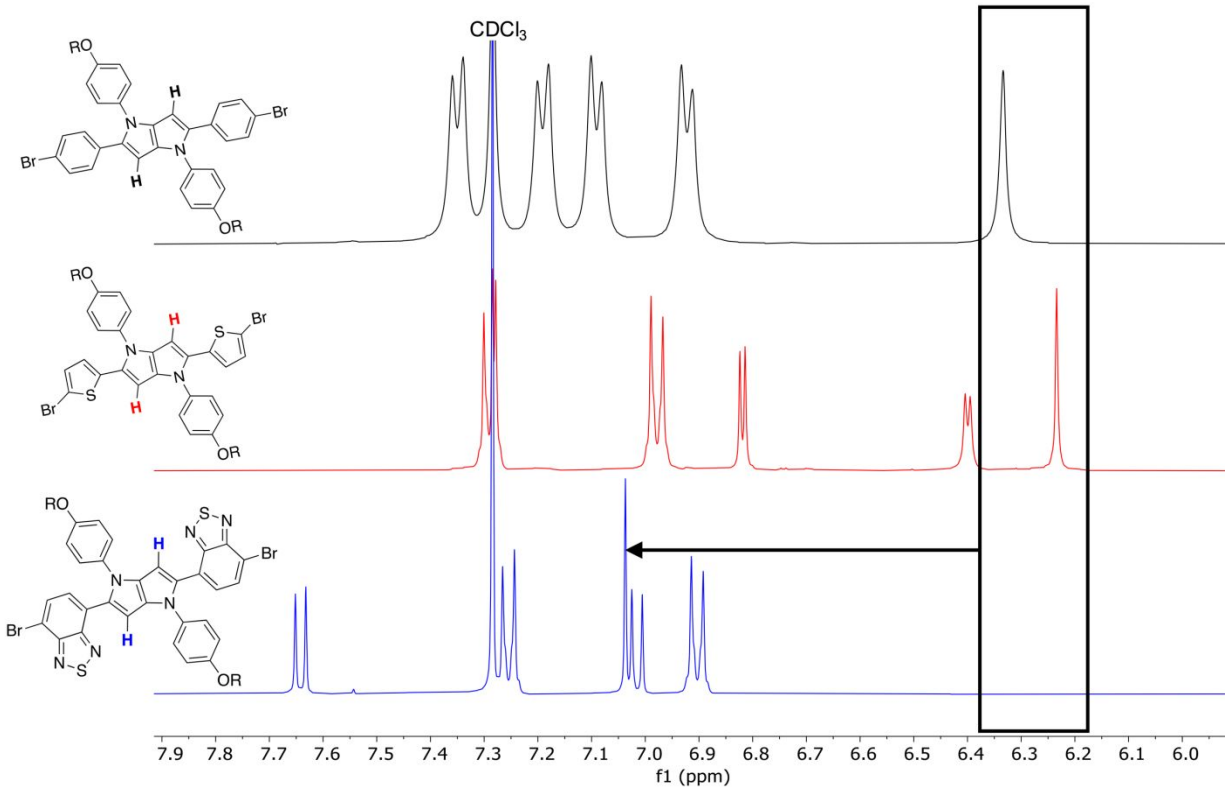

Figure 2. Aromatic region of ^{1}H NMR showing the changes in shielding effects for Ph_2DHPP (black), Th_2DHPP (red), and BTD_2DHPP (blue).

Motivated by the propensity of DHPP scaffolds to participate in Pd-catalyzed cross-coupling reactions and polymerizations, in addition to our successes synthesizing biphenyl DHPP chromophores, the brominated monomers were subjected Pd-catalyzed Suzuki polymerization protocols using bis(pinacolato)diboron as a comonomer and $Pd(PPh_3)_2Cl_2$ as the palladium source (Scheme 1(B)). The monomers and catalyst were heated at 110 °C in a 4:1 toluene/K_2CO_3(aq) solvent mixture under an argon (Ar) atmosphere. After purification via Soxhlet washes with

methanol (MeOH) and acetone, the polymers were extracted with chloroform. Both Ph_2DHPP and Th_2DHPP were collected with respectable yields of 70% and 77%, respectively, while yields for BTD_2DHPP were ~53% due to a large fraction of insoluble material remaining in the Soxhlet thimble. Each polymer retained their respective diagnostic peaks in their resulting NMR spectra but the line broadening and new chemical shifts corresponding to protons on the peripheral aromatic units in Figures S9-S11 support successful coupling. The number-average molecular weight (M_n) for Ph_2DHPP and Th_2DHPP were estimated to be 12.0 and 14.0 kg/mol, respectively, via size-exclusion chromatography (SEC) versus polystyrene standards using $CHCl_3$ as the eluent. Both polymers have a monomodal SEC traces and dispersity values ($Đ = M_w/M_n$) of 1.6 for Ph_2DHPP and 2.1 for Th_2DHPP (Figure S12 and S13). Solubility constraints for BTD_2DHPP inhibited molecular weight estimations due to the inability for BTD_2DHPP to pass through a GPC prefilter, even when using trichlorobenzene at elevated temperatures. However, as shown in Figure S14, there is a significant red shift in the absorbance of the BTD polymer compared to the BTD monomer which supports successful coupling and extending the π-conjugation. Due to the appreciable molecular weights and gaussian molecular weight distributions for Ph_2DHPP and Th_2DHPP, we are confident an adequate number of aromatic rings have been enchained to reach the effective conjugation length (ECL) for BTD_2DHPP and enable accurate elucidation of structure-property relationships.

The synthetic complexity for each polymer was calculated using Equation S1 and the results are tabulated in Table S1.[6] Ph_2DHPP has the lowest synthetic complexity of 14.5 followed by Th_2DHPP (20.9) and then BTD_2DHPP (22.5). The higher synthetic complexity for Th_2DHPP and BTD_2DHPP compared to Ph_2DHPP is attributed to the lower yields during monomer synthesis

but each polymer is still calculated to be more synthetically simple than many conjugated polymers.[36,37]

Optical Properties and Structural Analysis

To begin understanding the influence of repeat unit composition on optical properties, absorbance spectra for each polymer dissolved in toluene were measured with UV-vis absorbance spectroscopy. As shown by the solid traces in Figure 3 and reported in Table 1, there are distinct differences in the absorbance properties dependent on the choice of peripheral aromatic unit. First, Ph_2DHPP absorbs in the high energy portion of the electromagnetic spectrum with an absorbance maximum (λ_{max}) ~430 nm. This absorbance of Ph_2DHPP is slightly blue-shifted compared to the ProDOT-containing DHPP copolymer we reported in 2022 that had λ_{max} of 450 nm. Th_2DHPP and BTD_2DHPP show the expected red-shifted absorbance profiles with Th_2DHPP having a $\lambda_{max} \approx 515$ nm and BTD_2DHPP having a λ_{max} measured to be ~630 nm. The extended red shift measured for BTD_2DHPP is attributed to the electron-deficient nature of the BTD units coupled to the electron-rich DHPP core where a donor-acceptor (D-A) motif is attained that facilitates intramolecular charge transfer (ICT) transitions. While not entirely clear in the experimental measurement range (325 – 800 nm), there appears to be a high energy transition ~325 nm that would arise from the dual-band absorbance characteristics commonly associated with D-A polymers. All three polymers display featureless absorbance profiles in solution, which is indicative of the polymers being well-solvated without any noticeable vibronic features that would arise if there were increased levels of aggregation between polymer chains.

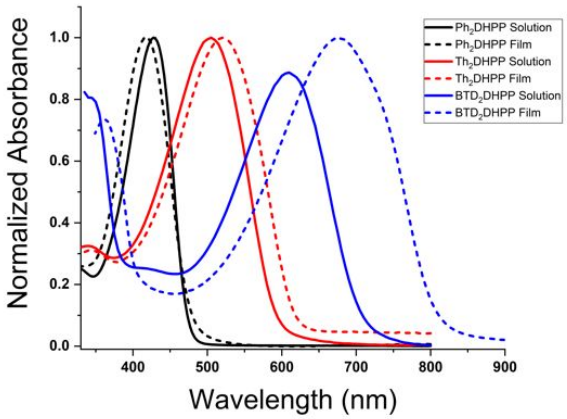

Figure 3. UV-vis absorbance spectra of Ph_2DHPP (black), Th_2DHPP (red), and BTD_2DHPP (blue) dissolved in toluene (solid) and as thin films (dashed).

Table 1. Optoelectronic and thermal properties of the DHPP-containing polymers reported in this manuscript.

Polymer	λ_{max}^{soln} **(nm)**	λ_{max}^{film} **(nm)**	E_{onset}^{ox} **(V)**	T_d **(°C)**
Ph_2DHPP	430	420	0.85	424
Th_2DHPP	515	540	0.70	412
BTD_2DHPP	630	725	1.0	318

Turning to computation for a deeper understanding of optical properties, frequency-verified optimization followed by excited state generation at the mPW3PBE/SV level was performed and the geometries and excited states of this set of systems were analyzed.[50–52] This level of theory was chosen due to the ability to accurately relate theory to experimental data while avoiding deficiencies of other functionals, such as the localization/delocalization error associated with the B3LYP global hybrid functional.[53] Initial analysis of the dihedral angles for each polymer are shown in Figure 4 where starting from the center (D_3) and then stepping to the peripheral rings shows that the Ph_2DPP is the most twisted out-of-plane while the Th_2DHPP and BTD_2DHPP are perfectly planar where the two subunits connect. For D_4 and D_2, planarity increases going from Ph_2DHPP to Th_2DHPP to BTD_2PHDD. It is only when analyzing D_1 and D_5 at the outer edges of

the oligomer, which would be analogous to polymer chain ends, that the contortion out-of-plane changes between Th_2DHPP (most planar) and BTD_2DHPP (least planar). Overall, the geometry is consistent with the trends measured by the experimental UV-Vis where Ph_2DPP (least planar, $\lambda_{max,DFT}$ = 414 nm) is more blue-shifted than Th_2DHPP ($\lambda_{max,DFT}$ = 524 nm) and then BTD_2DHPP (most planar, $\lambda_{max,DFT}$ = 838 nm).

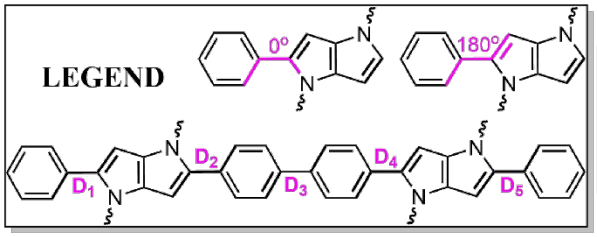

	D_1	D_2	D_3	D_4	D_5
Ph_2DPP	146°	147°	147°	147°	146°
Th_2DHPP	152°	155°	180°	155°	152°
BTD_2DHPP	138°	160°	179°	160°	138°

Figure 4. The five dihedral angles (D_1-D_5) are shown for each of the 3 DHPP oligomers constructed for modeling and elucidation of structural properties.

Examination of the frontier molecular orbitals (FMOs) enables identifying the type of excited state transition from which the absorption peak maximum arises (Figure 5). Both Ph_2DHPP and Th_2DHPP show only a slight reorganization of electron density from the highest occupied molecular orbital (HOMO) to lowest unoccupied molecular orbital (LUMO), which is indicative of a local excitation. Alternatively, BTD_2DHPP shows a more significant electronic redistribution in which the HOMO electron densities are evenly dispersed along the backbone while electron density in the LUMO is absent from the DHPP units and localized on the BTD rings. This trend is expected due to the electron-accepting nature of BTD coupled with the electron-donating DHPP that would produce a charge transfer type of excitation through the donor-acceptor approach. This behavior is further supported by the calculated energy gaps and oscillator strengths which were similar for Ph_2DHPP and Th_2DHPP but reduced nearly by half (relative to Ph_2DHPP) for BTD_2DHPP. The much narrower band gap is another indicator of BTD_2DHPP as a donor-acceptor motif and supports the experimental absorbance results reported above.

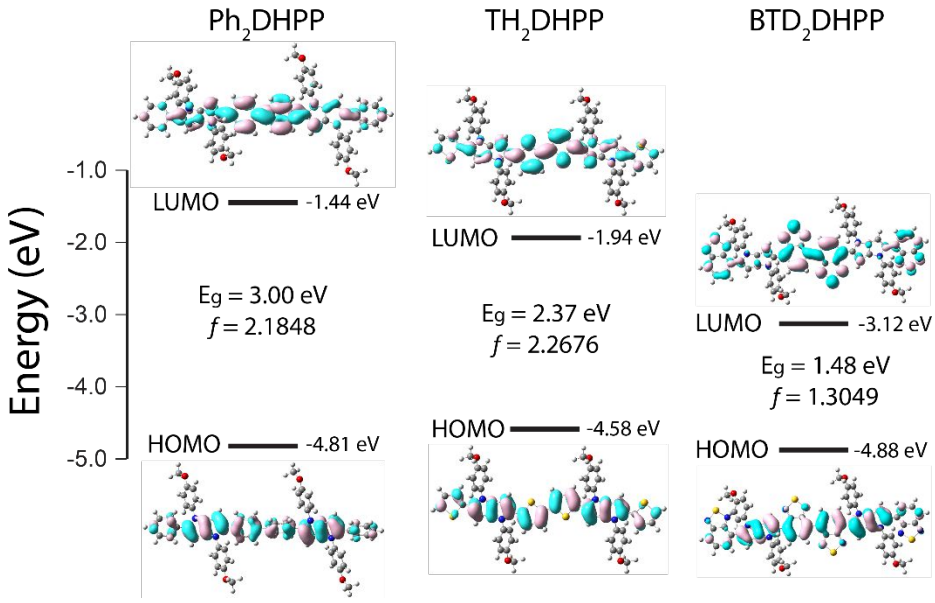

Figure 5. The energy band diagrams of the HOMO and LUMO levels for Ph_2DHPP, Th_2DHPP, and BTD_2DHPP are shown with corresponding frontier molecular orbital diagrams, optical gaps (E_g) and oscillator strengths (f).

Turning to studying the optical properties of these materials in the solid state, each polymer was dissolved in toluene, solution-processed into thin films via spin-coating, and had their absorbance measured. Th_2DHPP and BTD_2DHPP display the characteristic red-shifted absorbance associated for polymer as thin films when compared to dissolved in a solvent (dashed lines in Figure 3). This red shift is attributed to a larger degree of π-orbital overlap as well as an increased planarization of the polymer backbone in the solid state compared to solvated in solution. BTD_2DHPP shows the lowest onset of absorbance (λ_{onset}) ~820 nm and a λ_{max} ~725 nm while the Th_2DHPP λ_{onset} begins ~630 nm and the λ_{max} shifts to 540 nm. Alternatively, Ph_2DHPP unexpectedly showed a blue shift in the absorbance spectrum from 430 nm to 420 nm. Polymers containing DHPP units flanked by phenyl substituents are known to have minimal changes in their optical properties going from solution to thin films, which has been attributed to the larger dihedral angles through the polymer backbone preventing efficient interchain packing, but the blue-shifted absorbance warranted further probing to understand this phenomenon.

Our initial intuition leading to the blue-shifted absorbance was the polymer was "trapped" in an unfavorable morphology, perhaps due to processing protocols used to produce films of Ph_2DHPP. If this were the case, we suspected the blue shift would be corrected or reversed by annealing films at elevated temperatures. However, as shown in Figure S15, after annealing at 100 °C for 1 h, there were no discernable changes in the absorbance maxima. This led us to believe the blue shift is attributed to an unexpected aggregate phenomenon. To confirm the formation of aggregates, we chose to measure the absorbance of Ph_2DHPP in solution with varying concentrations of a poor solvent (MeOH) and monitor for any changes in the absorbance. Excitingly, our intuition was confirmed that increasing amounts of poor solvent would lead to changes in the absorbance spectra (Figure 6(A)), evident by measuring a 10 nm blue shift in 50% (v:v) toluene:MeOH solvent mixture. Qualitative fluorescence observations, shown as the photograph in the inset of Figure 6, also support the formation of aggregates due to increased quenching of the emission with increasing MeOH caused by aggregation-induced quenching.[54,55] The absorbance spectrum for the polymer aggregated in solution was plotted with the absorbance spectrum of Ph_2DHPP as a thin film (Figure 6(B)) and the two absorbance profiles are nearly identical. This data indicates that the blue shift measured going from solution to film is attributed to the formation of the same aggregate species formed during solution titration experiments.

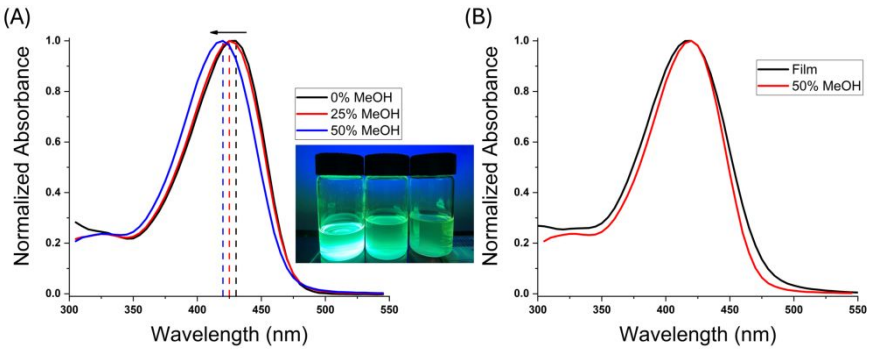

Figure 6. (A) UV-vis absorbance spectra of Ph_2DHPP in toluene solutions with varying fractions of MeOH as a poor solvent. The photograph in the inset shows the emission intensities of the same

solutions irradiated with UV light. (B) Overlayed UV-vis absorbance spectra of Ph_2DHPP as a thin film (black) and in a 50% toluene:MeOH solution (red). The near identical spectra are indicative of similar aggregation effects in solutions with poor solvent and as dried films.

Thermal Properties

Given the history of DHPP molecules and polymers finding applicability in organic electronic applications and devices, the thermal stability of Ph_2DHPP, Th_2DHPP, and BTD_2DHPP were studied using thermal gravimetric analysis (TGA). Ph_2DHPP showed the highest thermal stability with a degradation temperature (T_d) of 424 °C, followed by Th_2DHPP (T_d = 412 °C), and finally BTD_2DHPP (T_d = 318 °C). The mass loss at T_d for each polymer corresponds to the loss of the hexyldecyl sidechains attached to the 1,4-phenyl groups on the DHPP (Figure S16). Thermal properties were further probed via differential scanning calorimetry (DSC) to elucidate any thermal transitions (i.e T_g or T_m). As shown in Figure S17, Th_2DHPP and BTD_2DHPP do not display any distinct thermal transitions in the experimental window (-25 °C – 250 °C), which is analogous to previous iterations of DHPP-containing copolymers. Alternatively, Ph_2DHPP seems to have a small melting transition just over 100 °C and a corresponding crystallization (T_c) transition ~70 °C upon cooling. The observation of this deviation from other DHPP polymer systems is ostensibly due to the aggregation phenomenon described during UV-vis absorbance experiments that lead to the formation of small, but not insignificant, crystalline regions in bulk Ph_2DHPP samples.

Redox and Spectroelectrochemical Properties

The redox properties of the DHPP polymers as thin films were measured via cyclic voltammetry (CV). Films were created by drop-casting 2 mg/mL polymer solutions dissolved in toluene onto a glassy carbon electrode. CV results reported in Figure 7 show that Ph_2DHPP has an onset of oxidation (E_{onset}^{ox}) ~0.85 V (vs. Ag/AgCl in 0.5 M $TBAPF_6$/acetonitrile (ACN) supporting electrolyte), which is slightly higher than our ProDOT-containing DHPP copolymer due to the

removal of the electron-rich dioxythiophene motif. When the Ph units are replaced with flanking thiophenes, the E_{onset}^{ox} is lowered to ~0.7 V. This reduction in potential is attributed to the more electron rich nature, higher degree of planarization, and more quinoidal character of the thiophene unit compared to benzene. When the BTD unit is the flanking moiety, the E_{onset}^{ox} is increased to ~1.0 V vs Ag/AgCl which is attributed to the strong acceptor character of the BTD deepening the highest occupied molecular orbital (HOMO) compared to Th and Ph. All three polymers show a corresponding reduction process after oxidation with varying degrees of stability (*vide infra*).

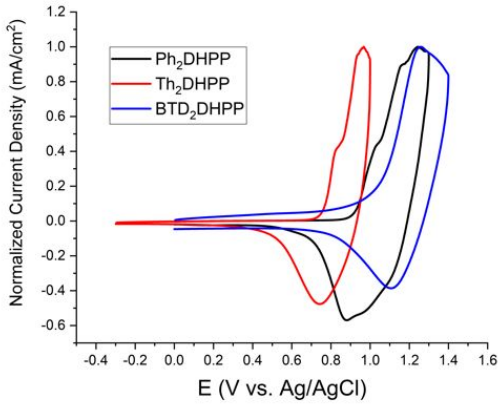

Figure 7. CV traces depicting the redox response for Ph_2DHPP (black), Th_2DHPP (red), and BTD_2DHPP (blue) as films deposited onto glassy carbon electrodes. Measurements were performed using a 0.5 M $TBAPF_6$/ACN supporting electrolyte and the Ag/AgCl reference electrode.

DHPP-based polymers and molecules have shown the ability for these systems to serve as active-layer material for multi-colored and high-contrast electrochromics[35,36,39] which necessitates studying the redox stability of the polymers reported in this study. While BTD_2DHPP shows an accompanying reduction for the redox process during the first redox cycle, films quickly degrade (within 5 cycles) which is not uncommon for D-A and *n*-type conjugated polymers studied as electrochromes. As shown in Figure 8(A), Ph_2DHPP also shows depleting redox activity over 10 cycles, although not as drastic as BTD_2DHPP. The decreasing redox activity for Ph_2DHPP is not surprising since our ProDOT-containing polymer showed an approximate 25% decrease in

electrochromic contrast with repeated electrochemical switching.[36] Additionally, phenylene-based polymers studied as electrochromic polymers are likely susceptible to undesired side reactions upon oxidation[40] and have shown lower switching stability. Th_2DHPP, on the other hand, shows excellent redox stability with extended electrochemical switching experiments. As shown in Figure 8(B), Th_2DHPP shows no signs of diminishing redox activity after 400 CV cycles and the only changes in the CV profiles is a result of "electrochemical annealing",[56,57] where the shape of CV traces will change over time due to the flux of solvent and ions in through the film. Overall, BTD_2DHPP and Ph_2DHPP may be suited for redox applications where a single switch or a small number of switches is needed while Th_2DHPP represents a design motif that has overcome stability issues of DHPP-containing polymers used in redox-active applications.

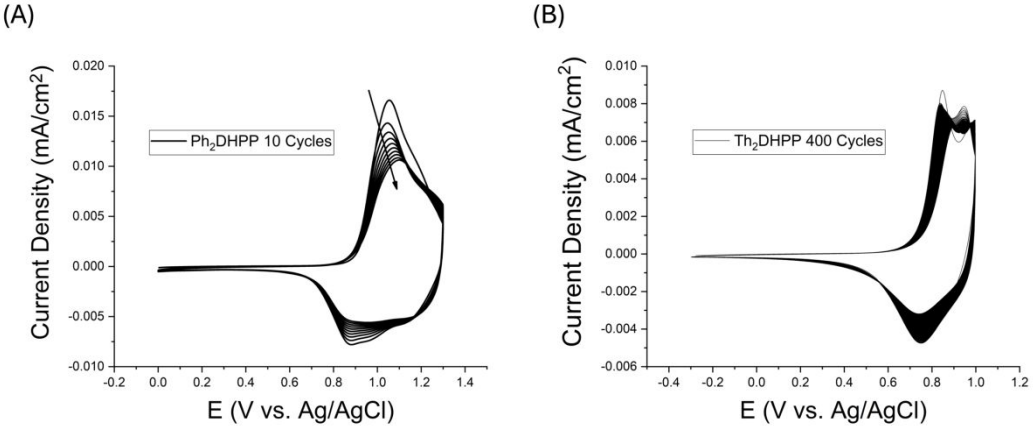

Figure 8. Redox response of (A) Ph_2DHPP and (B) Th_2DHPP upon repeated electrochemical sweeping cycles. Measurements were performed using a 0.5 M $TBAPF_6$/ACN supporting electrolyte and the Ag/AgCl reference electrode.

Changes in absorbance with increasing electrochemical potential was used to gain insights into charge-carrier formation of each polymer. While donor-acceptor type polymers have exhibited spectral changes with changing electrochemical potential, BTD_2DHPP did not show a spectroelectrochemical response upon oxidation[58] or reduction[59,60] but did show some spectral features that are worth noting. First, attempts at electrochemical conditioning led to diminished

absorbance (~50%) if swept in the cathodic (oxidation first) direction. However, as shown in Figure S18, the absorbance was maintained when sweeping towards negative potentials (reduction) first. Scanning in the reduction direction first also led to increased cycling stability of the polymer during CV experiments (Figure S19). However, without the accompanying reduction sweep, the electrochemical response once again rapidly diminished during attempts at oxidizing and measuring spectroelectrochemical response (Figure S20).

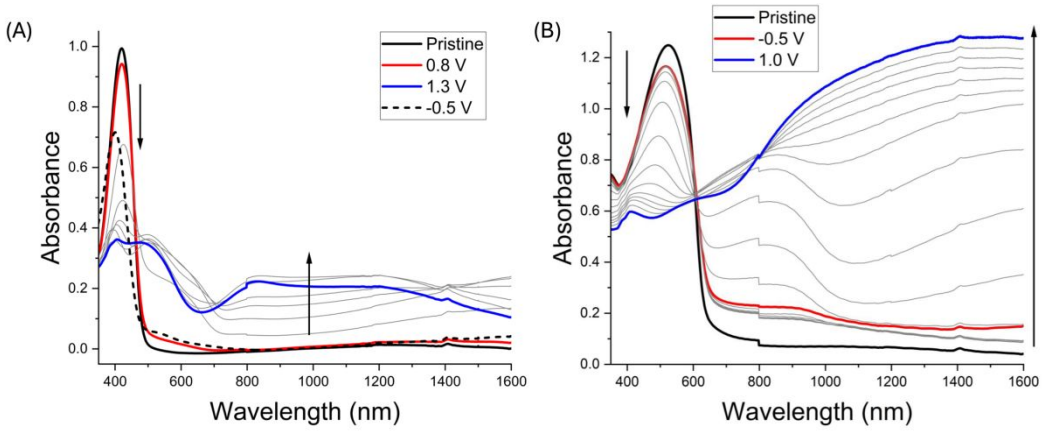

Figure 9. Absorbance spectra as a function of electrochemical potential for (A) Ph_2DHPP and (B) Th_2DHPP films that were processed via spray-casting from 5 mg/mL toluene solutions by applying varying potentials in 0.5 M $TBAPF_6$/ACN electrolyte.

Turning to the phenyl- and thienyl-containing polymers, potential-dependent absorbance spectra are presented in Figure 9. The polymer Ph_2DHPP shows a noticeable decrease in the absorbance ~ 0.8 V which corresponds to the onset of oxidation measured via CV. Similar to our first generation DHPP-containing copolymer, Ph_2DHPP retains significant absorbance across the visible spectrum upon oxidation but the absorbance features in the near-IR are less intense. Finally, the electrochemical instability observed in CV experiments is confirmed spectroscopically by measuring a blue-shifted and decreased absorbance of a Ph_2DHPP film after attempting to reduce the polymer back to a neutral state. Alternatively, the Th_2DHPP polymer demonstrated signs of efficient electrochemical doping. As shown in Figure 9(b), a neutral Th_2DHPP film transitions

from absorbing ~550 nm to the IR with increasing electrochemical potential. While the optical contrast of these films do not match the contrasts of dioxythiophene-type polymers, Th_2DHPP shows a full transition from the neutral to doped state similar to P3HT (Figure S21). These results suggest that Th_2DHPP possesses semiconducting properties based on the ability to transition from an insulating neutral polymer to a conductive polymer in its doped form.

To develop a deeper understanding of the optical transitions for electrochemically doped DHPP polymers, DFT calculations at the mPW3PBE/SV level followed by a time-dependent (TDDFT) treatment were performed for the radical cation forms of Ph_2DHPP and Th_2DHPP (BTD_2DHPP does not switch and as such was not included). To this end, the type of excitation may be identified through a study of electron distribution changes between the molecular orbitals involved in the excitation transition. A local excitation presents as small changes in electron distribution with mostly delocalized molecular orbitals. On the other hand, a charge transfer excitation will display redistribution of electron density from one region of the molecule to another. Figure 10 shows the FMOs for the two systems as well as their corresponding transition levels and excited state oscillator strengths. In the case of Ph_2DHPP, the strongest transition resulted from the $SOMO_\alpha$ to $LUMO_\alpha$ with an oscillator strength of 1.0600 and a peak maximum of 528 nm. There is a small redistribution of electron density from the periphery to the center which is indicative of some charge transfer character for this SOMO to LUMO transition. For Th_2DHPP, the $SOMO_\alpha$ to $LUMO_\alpha$ was red-shifted by 76 nm (528 nm versus 604 nm, Figures S25 and S29) and possessed a nearly doubled oscillator strength (1.0600 versus 2.0932) compared to Ph_2DHPP but the FMO pattern was similar to Ph_2DHPP and indicative of charge transfer character. Notably, the calculations agree with the trends observed from spectroelectrochemical measurements where

Th_2DHPP absorbs more strongly (i.e. larger oscillator strength) than Ph_2DHPP and transitions to longer wavelengths upon electrochemical doping.

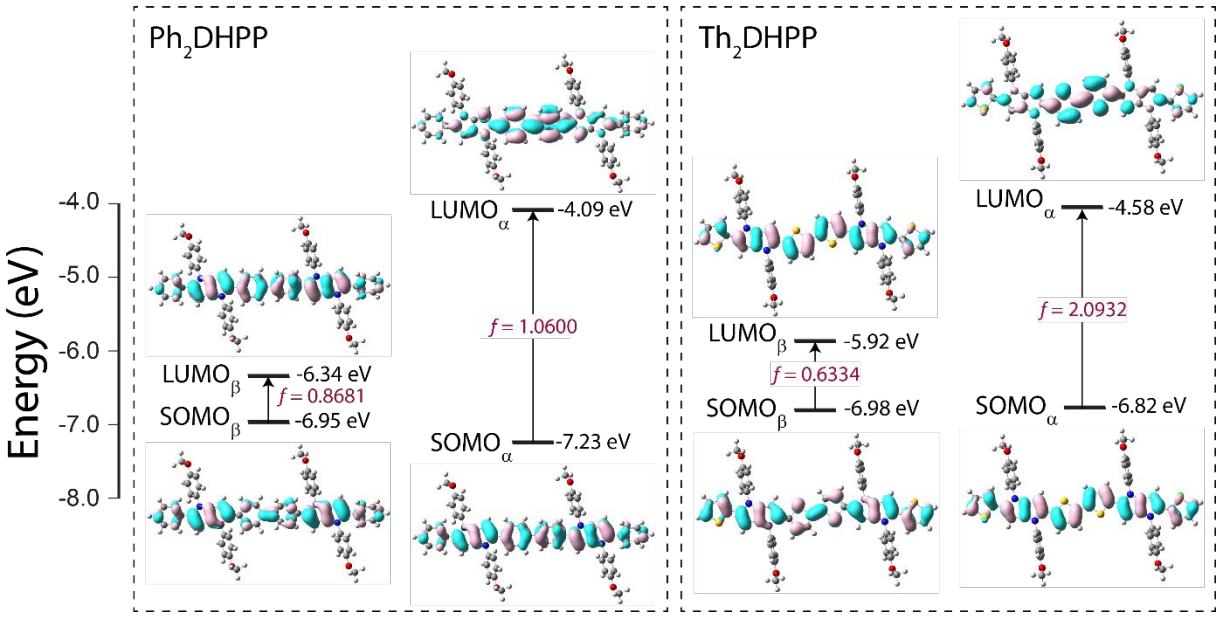

Figure 10. The lowest lying and most significant excited states are shown where the identity and energy of the original level and final level are provided as well as the corresponding FMO for each. The oscillator strengths (*f*) and arrow are provided for each of the individual excited states for clarity.

Conclusions

Pyrrolo[3,2-*b*]pyrroles are useful scaffolds that can be exploited for creating π-conjugated materials with tailorable optoelectronic properties from simple synthetic protocols. Their propensity to participate in Pd-catalyzed polymerizations enables these attributes to be expanded to polymeric materials and study the resulting structure-property relationships. As a way to expand the monomer toolbox, three DHPP monomers – *m*-Ph_2DHPP, *m*-Th_2DHPP, and *m*-BTD_2DHPP – were synthesized via aerobic Fe-catalyzed reactions between functionalized anilines and the corresponding aldehydes in the presence of 2,3-butanedione and purified without using column chromatography. The monomers were polymerized via Suzuki cross-coupling polymerizations to yield a novel class of synthetically simple conjugated polymers with tunable properties. The absorbance spectra for Th- and BTD-containing polymers are red-shifted compared to the Ph-

containing polymer due to increased planarity and ICT character, respectively. The choice of the peripheral aromatic unit also has drastic effects on the electrochemical properties of the resulting polymers, where the Th-containing polymer demonstrates superior redox stability and the ability to switch between doped and dedoped states. DFT calculations and analysis of FMOs support experimental measurements and provides insight into structural influences on optical properties of neutral and oxidized materials. Furthermore, thermal analyses show that the DHPP polymers are thermally stable and amenable to thermal treatment techniques commonly used for organic electronic applications. The large number of commercially-available aldehyde building blocks and synthetic transformations used to access aromatic aldehydes suggests DHPP-based polymers may be further functionalized for desired applications. Overall, these findings reinforce the utility of DHPPs as a highly-tailorable building block for conjugated materials and suggests these materials may find applicability in high-performance organic electronic devices.

Experimental and Computational Methodology

Comprehensive details of the experimental approaches are assembled and reported in the Supporting Information. Structure and connectivity of synthesized molecules and polymers were confirmed via ^{1}H and ^{13}C NMR. Full characterization including, NMR, elemental analysis, and size-exclusion chromatography (SEC) data can be found in the Supporting Information. To prepare spray-coated films, polymers were dissolved in toluene with a concentration of 2 mg/mL before deposition onto ITO-coated glass slides with an Iwata airbrush. Electrochemical and spectroelectrochemical measurements performed on the films used an electrolyte solution of 0.5 M tetrabutylammonium hexafluorophosphate ($TBAPF_6$) in propylene carbonate (PC), ITO/glass (7 × 50 × 0.7 mm, sheet resistance, R_s 8−12 Ω/sq) as the working electrode, an Ag/AgCl reference

electrode (calibrated versus the Fc/Fc^+ redox couple, $E_{1/2}$ = 46 mV), and a Pt flag as the counter electrode.

All systems were geometry optimized and frequency verified at the mPW3PBE level in gas phase. Excited states were generated through a time-dependent density functional theory (TDDFT) treatment for the lowest lying 15 excited states. The Cartesian coordinates of the optimized geometries, energy levels, a table of the lowest lying excited states with energy, oscillator strength, most significant transition and the percent this transition contributes to the excited state, geometric images and simulated UV-Vis spectra are provided for each system in the Supplemental Information.

Author Information

Corresponding Author

*E-mail graham.collier@usm.edu

Supporting Information

Detailed synthetic protocols, materials and methods, ^1H and ^{13}C NMR spectra, supporting spectroscopic, electrochemical, and electronic data.

Notes

The authors have no conflicts to declare.

Acknowledgements

This material is based upon work supported by the National Science Foundation under Grants No. 2448404. The authors acknowledge funding from the Department of Chemistry and Biochemistry at Kennesaw State University and the University of Southern Mississippi for start-up funds. Kennesaw State University Academic Affairs for support of the NMR facility, which made possible the research necessary for the completion of this project. The computations in this work used the Expanse Cluster at San Diego Supercomputer Center through allocation

DMR160146 from the Advanced Cyberinfrastructure Coordination Ecosystem: Services & Support (ACCESS) program, which is supported by U.S. National Science Foundation grants #2138259, #2138286, #2138307, #2137603, and #2138296.

References

(1) Zhang, G.; Lin, F. R.; Qi, F.; Heumüller, T.; Distler, A.; Egelhaaf, H.-J.; Li, N.; Chow, P. C. Y.; Brabec, C. J.; Jen, A. K.-Y.; Yip, H.-L. Renewed Prospects for Organic Photovoltaics. *Chem Rev* **2022**, *122* (18), 14180–14274. https://doi.org/10.1021/acs.chemrev.1c00955.

(2) Zou, S.-J.; Shen, Y.; Xie, F.-M.; Chen, J.-D.; Li, Y.-Q.; Tang, J.-X. Recent Advances in Organic Light-Emitting Diodes: Toward Smart Lighting and Displays. *Mater Chem Front* **2020**, *4* (3), 788–820. https://doi.org/10.1039/C9QM00716D.

(3) Li, X.; Perera, K.; He, J.; Gumyusenge, A.; Mei, J. Solution-Processable Electrochromic Materials and Devices: Roadblocks and Strategies towards Large-Scale Applications. *J. Mater. Chem. C* **2019**, *7* (41), 12761–12789. https://doi.org/10.1039/C9TC02861G.

(4) Ohayon, D.; Inal, S. Organic Bioelectronics: From Functional Materials to Next-Generation Devices and Power Sources. *Adv Mater* **2020**, *32* (36), 2001439. https://doi.org/10.1002/adma.202001439.

(5) Osedach, T. P.; Andrew, T. L.; Bulović, V. Effect of Synthetic Accessibility on the Commercial Viability of Organic Photovoltaics. *Energy Environ. Sci.* **2013**, *6* (3), 711–718. https://doi.org/10.1039/C3EE24138F.

(6) Po, R.; Bianchi, G.; Carbonera, C.; Pellegrino, A. "All That Glisters Is Not Gold": An Analysis of the Synthetic Complexity of Efficient Polymer Donors for Polymer Solar Cells. *Macromolecules* **2015**, *48* (3), 453–461. https://doi.org/10.1021/ma501894w.

(7) Moser, M.; Wadsworth, A.; Gasparini, N.; McCulloch, I. Challenges to the Success of Commercial Organic Photovoltaic Products. *Adv. Energy Mater.* **2021**, *11* (18), 2100056. https://doi.org/10.1002/aenm.202100056.

(8) Zhao, F.; Zhou, J.; He, D.; Wang, C.; Lin, Y. Low-Cost Materials for Organic Solar Cells. *J. Mater. Chem. C* **2021**, *9* (43), 15395–15406. https://doi.org/10.1039/D1TC04097A.

(9) Pappenfus, T. M.; Almyahi, F.; Cooling, N. A.; Culver, E. W.; Rasmussen, S. C.; Dastoor, P. C. Exploration of the Direct Arylation Polymerization Method for the Practical Application of Conjugated Materials: Synthetic Scale-Up, Solar Cell Performance, and Cost Analyses. *Macromol. Chem. Phys.* **2018**, *219* (21), 1800272. https://doi.org/10.1002/macp.201800272.

(10) Kleinschmidt, A. T.; Root, S. E.; Lipomi, D. J. Poly(3-Hexylthiophene) (P3HT): Fruit Fly or Outlier in Organic Solar Cell Research? *J. Mater. Chem. A* **2017**, *5* (23), 11396–11400. https://doi.org/10.1039/C6TA08317J.

(11) Guo, X.; Cui, C.; Zhang, M.; Huo, L.; Huang, Y.; Hou, J.; Li, Y. High Efficiency Polymer Solar Cells Based on Oly(3-Hexylthiophene)/Indene-C70 Bisadduct with Solvent Additive. *Energy Environ. Sci.* **2012**, *5* (7), 7943–7949. https://doi.org/10.1039/C2EE21481D.

(12) Holliday, S.; Ashraf, R. S.; Wadsworth, A.; Baran, D.; Yousaf, S. A.; Nielsen, C. B.; Tan, C.-H.; Dimitrov, S. D.; Shang, Z.; Gasparini, N.; Alamoudi, M.; Laquai, F.; Brabec, C. J.; Salleo, A.; Durrant, J. R.; McCulloch, I. High-Efficiency and Air-Stable P3HT-Based Polymer Solar Cells

with a New Non-Fullerene Acceptor. *Nat. Commun.* **2016**, *7* (1), 11585. https://doi.org/10.1038/ncomms11585.

(13) Liu, Q.; Jiang, Y.; Jin, K.; Qin, J.; Xu, J.; Li, W.; Xiong, J.; Liu, J.; Xiao, Z.; Sun, K.; Yang, S.; Zhang, X.; Ding, L. 18% Efficiency Organic Solar Cells. *Sci. Bull.* **2020**, *65* (4), 272–275. https://doi.org/10.1016/j.scib.2020.01.001.

(14) Arroyave, F. A.; Richard, C. A.; Reynolds, J. R. Efficient Synthesis of Benzo[1,2-b:6,5-B′]Dithiophene-4,5-Dione (BDTD) and Its Chemical Transformations into Precursors for π-Conjugated Materials. *Org. Lett.* **2012**, *14* (24), 6138–6141. https://doi.org/10.1021/ol302704v.

(15) Zhong, X.; Chen, T.-W.; Yan, L.; You, W. Facile Synthesis of Key Building Blocks of D18 Series Conjugated Polymers for High-Performance Polymer Solar Cells. *ACS Appl. Polym. Mater.* **2023**, *5* (3), 1937–1944. https://doi.org/10.1021/acsapm.2c02009.

(16) Sun, C.; Pan, F.; Bin, H.; Zhang, J.; Xue, L.; Qiu, B.; Wei, Z.; Zhang, Z.-G.; Li, Y. A Low Cost and High Performance Polymer Donor Material for Polymer Solar Cells. *Nat. Commun.* **2018**, *9* (1), 743. https://doi.org/10.1038/s41467-018-03207-x.

(17) Li, S.; Zhan, L.; Sun, C.; Zhu, H.; Zhou, G.; Yang, W.; Shi, M.; Li, C.-Z.; Hou, J.; Li, Y.; Chen, H. Highly Efficient Fullerene-Free Organic Solar Cells Operate at Near Zero Highest Occupied Molecular Orbital Offsets. *J. Am. Chem. Soc.* **2019**, *141* (7), 3073–3082. https://doi.org/10.1021/jacs.8b12126.

(18) Sun, C.; Qin, S.; Wang, R.; Chen, S.; Pan, F.; Qiu, B.; Shang, Z.; Meng, L.; Zhang, C.; Xiao, M.; Yang, C.; Li, Y. High Efficiency Polymer Solar Cells with Efficient Hole Transfer at Zero Highest Occupied Molecular Orbital Offset between Methylated Polymer Donor and Brominated Acceptor. *J. Am. Chem. Soc.* **2020**, *142* (3), 1465–1474. https://doi.org/10.1021/jacs.9b09939.

(19) Rech, J. J.; Neu, J.; Qin, Y.; Samson, S.; Shanahan, J.; Josey III, R. F.; Ade, H.; You, W. Designing Simple Conjugated Polymers for Scalable and Efficient Organic Solar Cells. *ChemSusChem* **2021**, *14* (17), 3561–3568. https://doi.org/10.1002/cssc.202100910.

(20) Neu, J.; Samson, S.; Ding, K.; Rech, J. J.; Ade, H.; You, W. Oligo(Ethylene Glycol) Side Chain Architecture Enables Alcohol-Processable Conjugated Polymers for Organic Solar Cells. *Macromolecules* **2023**, *56* (5), 2092–2103. https://doi.org/10.1021/acs.macromol.2c02259.

(21) Rimmele, M.; Qiao, Z.; Panidi, J.; Furlan, F.; Lee, C.; Tan, W. L.; McNeill, C. R.; Kim, Y.; Gasparini, N.; Heeney, M. A Polymer Library Enables the Rapid Identification of a Highly Scalable and Efficient Donor Material for Organic Solar Cells. *Mater. Horiz.* **2023**, *10* (10), 4202–4212. https://doi.org/10.1039/D3MH00787A.

(22) Welsh, D. M.; Kumar, A.; Meijer, E. W.; Reynolds, J. R. Enhanced Contrast Ratios and Rapid Switching in Electrochromics Based on Poly(3,4-Propylenedioxythiophene) Derivatives. *Adv. Mater.* **1999**, *11* (16), 1379–1382. https://doi.org/10.1002/(SICI)1521-4095(199911)11:16<1379::AID-ADMA1379>3.0.CO;2-Q.

(23) Gaupp, C. L.; Welsh, D. M.; Reynolds, J. R. Poly(ProDOT-Et2): A High-Contrast, High-Coloration Efficiency Electrochromic Polymer. *Macromol. Rapid Commun.* **2002**, *23* (15), 885–889. https://doi.org/10.1002/1521-3927(20021001)23:15<885::AID-MARC885>3.0.CO;2-X.

(24) Bardagot, O.; DiTullio, B. T.; Jones, A. L.; Speregen, J.; Reynolds, J. R.; Banerji, N. Balancing Electroactive Backbone and Oligo(Ethylene Oxy) Side-Chain Content Improves Stability and Performance of Soluble PEDOT Copolymers in Organic Electrochemical Transistors. *Adv. Funct. Mater.* **2024**, *n/a* (n/a), 2412554. https://doi.org/10.1002/adfm.202412554.

(25) Estrada, L. A.; Deininger, J. J.; Kamenov, G. D.; Reynolds, J. R. Direct (Hetero)Arylation Polymerization: An Effective Route to 3,4-Propylenedioxythiophene-Based Polymers with Low Residual Metal Content. *ACS Macro Lett.* **2013**, *2* (10), 869–873. https://doi.org/10.1021/mz4003886.

(26) Collier, G. S.; Reynolds, J. R. Exploring the Utility of Buchwald Ligands for C–H Oxidative Direct Arylation Polymerizations. *ACS Macro Lett.* **2019**, *8* (8), 931–936. https://doi.org/10.1021/acsmacrolett.9b00395.

(27) Tarange, D. L.; Nayak, N.; Kumar, A. Continuous Flow Synthesis of Substituted 3,4-Propylenedioxythiophene Derivatives. *Org. Process Res. Dev.* **2023**, *27* (2), 358–366. https://doi.org/10.1021/acs.oprd.2c00356.

(28) Krzeszewski, M.; Gryko, D.; Gryko, D. T. The Tetraarylpyrrolo[3,2-b]Pyrroles—From Serendipitous Discovery to Promising Heterocyclic Optoelectronic Materials. *Acc. Chem. Res.* **2017**, *50* (9), 2334–2345. https://doi.org/10.1021/acs.accounts.7b00275.

(29) Tasior, M.; Koszarna, B.; Young, D. C.; Bernard, B.; Jacquemin, D.; Gryko, D.; Gryko, D. T. Fe(III)-Catalyzed Synthesis of Pyrrolo[3,2-b]Pyrroles: Formation of New Dyes and Photophysical Studies. *Org Chem Front* **2019**, *6* (16), 2939–2948. https://doi.org/10.1039/C9QO00675C.

(30) Tasior, M.; Vakuliuk, O.; Koga, D.; Koszarna, B.; Górski, K.; Grzybowski, M.; Kielesiński, Ł.; Krzeszewski, M.; Gryko, D. T. Method for the Large-Scale Synthesis of Multifunctional 1,4-Dihydro-Pyrrolo[3,2-b]Pyrroles. *J Org Chem* **2020**, *85* (21), 13529–13543. https://doi.org/10.1021/acs.joc.0c01665.

(31) Domínguez, R.; Montcada, N. F.; de la Cruz, P.; Palomares, E.; Langa, F. Pyrrolo[3,2-b]Pyrrole as the Central Core of the Electron Donor for Solution-Processed Organic Solar Cells. *ChemPlusChem* **2017**, *82* (7), 1096–1104. https://doi.org/10.1002/cplu.201700158.

(32) Wang, J.; Chai, Z.; Liu, S.; Fang, M.; Chang, K.; Han, M.; Hong, L.; Han, H.; Li, Q.; Li, Z. Organic Dyes Based on Tetraaryl-1,4-Dihydropyrrolo-[3,2-b]Pyrroles for Photovoltaic and Photocatalysis Applications with the Suppressed Electron Recombination. *Chem Euro J* **2018**, *24* (68), 18032–18042. https://doi.org/10.1002/chem.201803688.

(33) Zhou, Y.; Zhang, M.; Ye, J.; Liu, H.; Wang, K.; Yuan, Y.; Du, Y.-Q.; Zhang, C.; Zheng, C.-J.; Zhang, X.-H. Efficient Solution-Processed Red Organic Light-Emitting Diode Based on an Electron-Donating Building Block of Pyrrolo[3,2-b]Pyrrole. *Org Electron* **2019**, *65*, 110–115. https://doi.org/10.1016/j.orgel.2018.11.007.

(34) Hawes, C. S.; Ó Máille, G. M.; Byrne, K.; Schmitt, W.; Gunnlaugsson, T. Tetraarylpyrrolo[3,2-b]Pyrroles as Versatile and Responsive Fluorescent Linkers in Metal–Organic Frameworks. *Dalton Trans.* **2018**, *47* (30), 10080–10092. https://doi.org/10.1039/C8DT01784K.

(35) Hawks, A. M.; Daniel, L. M.; Sorto, V. S.; Mauro, J.; Skiouris, P.; Collier, G. S. Expanding Color Control of Anodically Coloring Electrochromes Based on Electron-Rich 1,4-

Dihydropyrrolo[3,2-b]Pyrroles. *ACS Appl Opt Mater* **2024**, *2* (6), 1235–1244. https://doi.org/10.1021/acsaom.4c00197.

(36) Bell, K.-J. J.; Kisiel, A. M.; Smith, E.; Tomlinson, A. L.; Collier, G. S. Simple Synthesis of Conjugated Polymers Enabled via Pyrrolo[3,2-b]Pyrroles. *Chem. Mater.* **2022**, *34* (19), 8729–8739. https://doi.org/10.1021/acs.chemmater.2c01884.

(37) Bell, K.-J. J.; Sabury, S.; Phan, V.; Wagner, E. M.; Hawks, A. M.; Bartlett, K. A.; Collier, G. S. Synthesis of 1,4-Dihydropyrrolo[3,2-b]Pyrrole-Containing Donor–Acceptor Copolymers and Their Optoelectronic Properties. *J Poly Sci* **2024**, *62*, 2975. https://doi.org/10.1002/pol.20240093.

(38) Bartlett, K. A.; Charland-Martin, A.; Lawton, J.; Tomlinson, A. L.; Collier, G. S. Azomethine-Containing Pyrrolo[3,2-b]Pyrrole Copolymers for Simple and Degradable Conjugated Polymers. *Macromol Rapid Commun* **2024**, *45* (1), 2300220. https://doi.org/10.1002/marc.202300220.

(39) Hawks, A. M.; Altman, D.; Faddis, R.; Wagner, E. M.; Bell, K.-J. J.; Charland-Martin, A.; Collier, G. S. Relating Design and Optoelectronic Properties of 1,4-Dihydropyrrolo[3,2-b]Pyrroles Bearing Biphenyl Substituents. *J Phys Chem B* **2023**, *127* (33), 7352–7360. https://doi.org/10.1021/acs.jpcb.3c03061.

(40) Cao, K.; Shen, D. E.; Österholm, A. M.; Kerszulis, J. A.; Reynolds, J. R. Tuning Color, Contrast, and Redox Stability in High Gap Cathodically Coloring Electrochromic Polymers. *Macromolecules* **2016**, *49* (22), 8498–8507. https://doi.org/10.1021/acs.macromol.6b01763.

(41) Górski, K.; Kusy, D.; Ozaki, S.; Banasiewicz, M.; Valiev, R.; Sahoo, S. R.; Kamada, K.; Baryshnikov, G.; Gryko, D. T. The Interplay of Intersystem Crossing and Internal Conversion in Quadrupolar Tetraarylpyrrolo[3,2-b]Pyrroles. *J. Mater. Chem. C* **2024**, *12* (6), 1980–1987. https://doi.org/10.1039/D3TC03851C.

(42) Canjeevaram Balasubramanyam, R. K.; Kumar, R.; Ippolito, S. J.; Bhargava, S. K.; Periasamy, S. R.; Narayan, R.; Basak, P. Quadrupolar (A-π-D-π-A) Tetra-Aryl 1,4-Dihydropyrrolo[3,2-b]Pyrroles as Single Molecular Resistive Memory Devices: Substituent Triggered Amphoteric Redox Performance and Electrical Bistability. *J Phys Chem C* **2016**, *120* (21), 11313–11323. https://doi.org/10.1021/acs.jpcc.5b11509.

(43) Santra, M.; Jun, Y. W.; Bae, J.; Sarkar, S.; Choi, W.; Gryko, D. T.; Ahn, K. H. Water-Soluble Pyrrolo[3,2-b]Pyrroles: Synthesis, Luminescence and Two-Photon Cellular Imaging Properties. *Asian J Org Chem* **2017**, *6* (3), 278–281. https://doi.org/10.1002/ajoc.201600613.

(44) Tasior, M.; Vakuliuk, O.; Wrzosek, A.; Vullev, V. I.; Szewczyk, A.; Jacquemin, D.; Gryko, D. T. Quadrupolar, Highly Polarized Dyes: Emission Dependence on Viscosity and Selective Mitochondria Staining. *ACS Org. Inorg. Au* **2024**, *4* (2), 248–257. https://doi.org/10.1021/acsorginorgau.3c00035.

(45) Tasior, M.; Kowalczyk, P.; Przybył, M.; Czichy, M.; Janasik, P.; Bousquet, M. H. E.; Łapkowski, M.; Rammo, M.; Rebane, A.; Jacquemin, D.; Gryko, D. T. Going Beyond the Borders: Pyrrolo[3,2-b]Pyrroles with Deep Red Emission. *Chem. Sci.* **2021**, *12* (48), 15935–15946. https://doi.org/10.1039/D1SC05007A.

(46) Górski, K.; Deperasińska, I.; Baryshnikov, G. V.; Ozaki, S.; Kamada, K.; Ågren, H.; Gryko, D. T. Quadrupolar Dyes Based on Highly Polarized Coumarins. *Org Lett* **2021**, *23* (17), 6770–6774. https://doi.org/10.1021/acs.orglett.1c02349.

(47) Teimouri, M. B.; Deperasińska, I.; Rammo, M.; Banasiewicz, M.; Stark, C. W.; Dobrzycki, Ł.; Cyrański, M. K.; Rebane, A.; Gryko, D. T. Strongly Polarized π-Extended 1,4-Dihydropyrrolo[3,2-b]Pyrroles Fused with Tetrazolo[1,5-a]Quinolines. *J. Org. Chem.* **2024**, *89* (7), 4657–4672. https://doi.org/10.1021/acs.joc.3c02916.

(48) Kowalczyk, P.; Tasior, M.; Ozaki, S.; Kamada, K.; Gryko, D. T. From 2,5-Diformyl-1,4-Dihydropyrrolo[3,2-b]Pyrroles to Quadrupolar, Centrosymmetric Two-Photon-Absorbing A–D–A Dyes. *Org. Lett.* **2022**, *24* (13), 2551–2555. https://doi.org/10.1021/acs.orglett.2c00718.

(49) Collier, G. S.; Brown, L. A.; Boone, E. S.; Kaushal, M.; Ericson, M. N.; Walter, M. G.; Long, B. K.; Kilbey, S. M. Linking Design and Properties of Purine-Based Donor–Acceptor Chromophores as Optoelectronic Materials. *J. Mater. Chem. C* **2017**, *5* (27), 6891–6898. https://doi.org/10.1039/C7TC01835E.

(50) Nhon, L.; Wilkins, R.; Reynolds, J. R.; Tomlinson, A. Guiding Synthetic Targets of Anodically Coloring Electrochromes through Density Functional Theory. *J. Chem. Phys.* **2021**, *154* (5), 054110. https://doi.org/10.1063/5.0039511.

(51) Tannir, S.; Chavez, R. I.; Molina, G. I.; Tomlinson, A.; Jeffries-EL, M. Evaluating the Effect of Extended Conjugation and Regioisomerism on the Optoelectronic Properties and Device Efficiencies of Blue Light-Emitting Benzobisoxazoles. *Chem. Mater.* **2024**, *36* (10), 4945–4954. https://doi.org/10.1021/acs.chemmater.3c02109.

(52) Wagner, J. S.; Siegler, M. A.; Tomlinson, A. L.; Reynolds, J. R. Controlling Charged State Colors in Triphenylamine-Based Anodically Coloring Electrochromes. *Adv. Opt. Mater.* **2024**, *12* (28), 2400855. https://doi.org/10.1002/adom.202400855.

(53) Körzdörfer, T.; Brédas, J.-L. Organic Electronic Materials: Recent Advances in the DFT Description of the Ground and Excited States Using Tuned Range-Separated Hybrid Functionals. *Acc. Chem. Res.* **2014**, *47* (11), 3284–3291. https://doi.org/10.1021/ar500021t.

(54) Xie, D.; Parthasarathy, A.; Schanze, K. S. Aggregation-Induced Amplified Quenching in Conjugated Polyelectrolytes with Interrupted Conjugation. *Langmuir* **2011**, *27* (19), 11732–11736. https://doi.org/10.1021/la202122p.

(55) Congrave, D. G.; Drummond, B. H.; Gray, V.; Bond, A. D.; Rao, A.; Friend, R. H.; Bronstein, H. Suppressing Aggregation Induced Quenching in Anthracene Based Conjugated Polymers. *Polym. Chem.* **2021**, *12* (12), 1830–1836. https://doi.org/10.1039/D1PY00118C.

(56) Heinze, J.; Frontana-Uribe, B. A.; Ludwigs, S. Electrochemistry of Conducting Polymers—Persistent Models and New Concepts. *Chem. Rev.* **2010**, *110* (8), 4724–4771. https://doi.org/10.1021/cr900226k.

(57) Collier, G. S.; Wilkins, R.; Tomlinson, A. L.; Reynolds, J. R. Exploring Isomeric Effects on Optical and Electrochemical Properties of Red/Orange Electrochromic Polymers. *Macromolecules* **2021**, *54* (4), 1677–1692. https://doi.org/10.1021/acs.macromol.0c02719.

(58) Beaujuge, P. M.; Amb, C. M.; Reynolds, J. R. Spectral Engineering in π-Conjugated Polymers with Intramolecular Donor−Acceptor Interactions. *Acc. Chem. Res.* **2010**, *43* (11), 1396–1407. https://doi.org/10.1021/ar100043u.

(59) Stalder, R.; Mei, J.; Graham, K. R.; Estrada, L. A.; Reynolds, J. R. Isoindigo, a Versatile Electron-Deficient Unit For High-Performance Organic Electronics. *Chem. Mater.* **2014**, *26* (1), 664–678. https://doi.org/10.1021/cm402219v.

(60) Andjaba, J. M.; Rybak, C. J.; Wang, Z.; Ling, J.; Mei, J.; Uyeda, C. Catalytic Synthesis of Conjugated Azopolymers from Aromatic Diazides. *J. Am. Chem. Soc.* **2021**, *143* (10), 3975–3982. https://doi.org/10.1021/jacs.1c00447.

Data Availability Statement

The data supporting this article have been included as part of the Supplementary Information